Liquid Crystals
Publication details, including instructions for authors and subscription information:
http://www.informaworld.com/smpp/title~content=t713926090

The use of a time resolved Raman microprobe to study the electric field induced Fréedericksz transition in the alkyl cyanobiphenyl homologues

K. M. Booth[ab]; H. J. Coles[a]
[a] Liquid Crystal Group, Physics Department, Manchester University, Manchester, England [b] Department of Pure and Applied Physics, University of Salford, Salford, England

To cite this Article Booth, K. M. and Coles, H. J.(1993) 'The use of a time resolved Raman microprobe to study the electric field induced Fréedericksz transition in the alkyl cyanobiphenyl homologues', Liquid Crystals, 13: 5, 677 — 690
To link to this Article: DOI: 10.1080/02678299308026340
URL: http://dx.doi.org/10.1080/02678299308026340

LIQUID CRYSTALS, 1993, VOL. 13, NO. 5, 677–690

The use of a time resolved Raman microprobe to study the electric field induced Fréedericksz transition in the alkyl cyanobiphenyl homologues

by K. M. BOOTH† and H. J. COLES*
Liquid Crystal Group, Physics Department, Manchester University, Oxford Road, Manchester, M13 9PL, England

(*Received 18 November 1991; accepted 23 January 1993*)

The bond selectivity of the Raman technique is exploited with a time resolved Raman microprobe to determine the effective splay viscosity coefficients and elastic constants in the nematic phase of the 4-*n*-alkyl-4-cyanobiphenyl homologues 5, 6, 7 and 8CB. The Raman effect, using the signal associated with the core and the flexible alkyl chains, was used to probe the Fréedericksz transition in the limit of small deformations. The data for the cores show good agreement with data published elsewhere. Odd–even effects were found and, in the case of 8CB, pretransitional effects due to the lower temperature S_A phase were observed. The viscosity data for the flexible alkyl chains, at a reduced temperature of 3°C, yield values for the apparent viscosity coefficients that are approximately half that of their respective rigid cores. This is considered to be indicative of the influence of the molecular flexibility on the effective director field. The data illustrate the usefulness of the technique for studying microscopic volumes of multicomponent systems.

1. Introduction

Raman spectroscopy is a technique that has seen a considerable revival of interest in the past 30 years following the advent of the laser and the original technique of spontaneous Raman scattering has been extended over the years so that, for example, there are now techniques for enhancing weak signals in the processes of resonance [1] and surface enhanced [2] Raman. Laser light may be amplified and tuned using the non-linear process of stimulated Raman scattering [3, 4]. Parallel improvements in data acquisition have led to the development of intensified diode arrays which allow the capture of an entire spectrum in milliseconds, and have further opened up ways of rejecting background noise due to fluorescence [5]. The use of Raman spectroscopy as a microanalytical tool was pioneered by the National Bureau of Standards in the U.S.A. and the Centre Nationale de la Recherche at Lille in France [6, 7]. In essence, the conventional illuminating and collecting optics are replaced by an adapted microscope assembly that gives a spatial resolution of microns. The small spot size and high power densities achievable illustrate a further advantage of the microprobe technique since it enables samples of micron dimensions to be studied, thus making it a suitable technique for the study of liquid crystal films which are only ten or so microns thick. One of us [8] recently reported a polarized Raman microprobe apparatus, which also enabled dynamic information to be recorded on the microsecond timescale with

* Author for correspondence.
† Present address: Department of Pure and Applied Physics, University of Salford, Salford, M5 4WT, England.

0267–8292/93 $10·00

the rejection of stray fluorescent signals. Herein we describe briefly an apparatus that maintains the advantages of the time resolved Raman microprobe system but with improved sensitivity.

A knowledge of the viscosity coefficients and elastic constants of nematic liquid crystals is of vital importance in their characterization since these control, for example, the operating parameters if the material is to be used in a device. There are a number of established methods for determining these, individually, on a macroscopic scale: quasi-elastic light scattering [9] Zvetkow shear viscometry [10] and Fréedericksz transition measurement [11], etc. Here the polarized time resolved Raman microprobe [12] is used to evaluate these parameters in microscopic volume samples using the bond selectivity of the technique to monitor signals associated with different sections of the molecule as they respond to an applied external field, i.e. in a Fréedericksz transition. These signals, which arise in the present work from molecular modes of vibration, probe a macroscopic nematic director and indeed may be used to measure $\langle P_2 \rangle$ and $\langle P_4 \rangle$ order parameters [13–17]. By using the site selectivity of the polarized Raman technique and the improved sensitivity of the time resolved microprobe we examine whether signals arising from different molecular sites give rise to different electrooptic signals. Thus is should be possible to monitor effects due to molecular flexibility. We have studied the nematogenic alkylcyanobiphenyls and it should be stressed that all data have been extracted in the limit of small deformations under the applied field in line with the Pieranski *et al.* [18] analysis which we use. A comparison is then made between this detailed data and that already determined theoretically and experimentally by well-known macroscopic techniques to evaluate the usefulness of the present method. Since the data for the alkylcyanobiphenyls are well documented their study gives us a particularly clear test of the new technique.

2. Theory

The change in the intensity of Raman scattered light from a thin nematic film (of thickness d) as a function of director orientation, $\mathbf{n}$ is shown schematically in figure 1. Initially the director is aligned parallel to the polarization direction of the incident light by using suitably treated surfaces to give a planar alignment. This gives a relatively strong Raman signal. As $\mathbf{n}$ moves away from the linear polarization direction of the incoming laser beam the Raman signal decreases. As depicted, $\mathbf{n}$ remains in the polarization plane of the incident beam and moves towards a homeotropic alignment in response to an applied low frequency electric field $\mathbf{E}$. In the limit of small distortions the intensity of the scattered light may be represented as [19]

$$I=(A_0+A_1+A_2)-(A_1+2A_2)\psi^2, \tag{1}$$

where A_0, A_1 and A_2 are constants related to the molecular tensor components. The theory of Pieranski *et al.* [18] relates the reorientation angle, ψ, as a function of time, to the physical parameters of the nematic system and the relative magnitude of the applied AC field. For the splay configuration and small distortions this may be written as

$$\psi_m^2(t)=\frac{\psi_m^2(\infty)}{1+\left[\dfrac{\psi_m^2(\infty)}{\xi^2}-1\right]\exp\left\{-\dfrac{2\varepsilon_0\Delta\varepsilon}{\eta_{splay}d^2}(V^2-V_c^2)t\right\}}, \tag{2}$$

where $\psi_m(\infty)$ is the maximum angle reached after time $t=\infty$ at the centre of the cell, ξ^2 is the time average [18] of the fluctuations of the orientation in the undisturbed state at

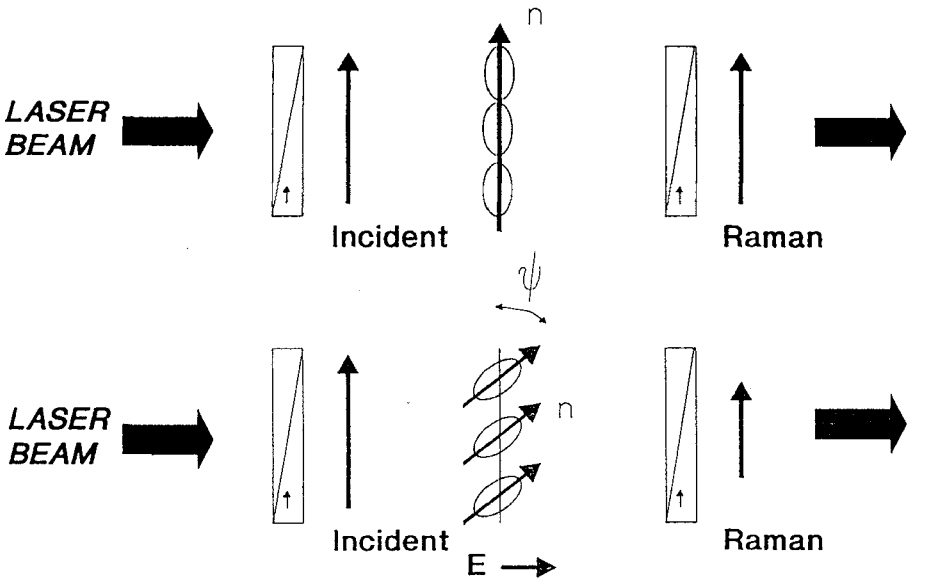

Figure 1. A schematic showing the effect of the director orientation, **n** on scattered Raman intensity. The **E** field is applied as shown and the nematic has $\Delta\varepsilon/0$. The height of the Raman arrows are indicative of light intensity changes (not to scale). The initial planar alignment (for $\mathbf{E}=0, t<0$) is obtained by rubbed surface alignment agents in a sample cell of thickness d.

$t=0$ (i.e. $\xi^2=\langle\psi_m^2(t=0)\rangle$), $\Delta\varepsilon$ is the anisotropy of the dielectric permittivity, η_{splay} is the splay viscosity coefficient, d is the cell thickness, V is the applied voltage and V_c is the critical voltage for the Fréedericksz transition (n.b. both are rms voltages).

Combining equations (1) and (2) the variation in scattered Raman intensity with time after a voltage V has been applied, and within the limit of small deformations, is of the form

$$I(t)=A-\frac{B}{1+C\exp(-St)}, \tag{3}$$

where A, B and C may be considered as constants for each given voltage and

$$S=\frac{2\varepsilon_0\Delta\varepsilon}{\eta_{splay}d^2}(V^2-V_c^2). \tag{4}$$

Further, k_{11}, the splay elastic constant, and V_c are related through

$$V_c=\pi\sqrt{\left(\frac{k_{11}}{\varepsilon_0\Delta\varepsilon}\right)}. \tag{5}$$

Thus by fitting equation (3) to the time dependence of the Raman signal, in the limit of small deformations (cf. equation (2)), on application of a low voltage V and by measuring V_c both η_{splay} and k_{11} may be determined, assuming $\Delta\varepsilon$ is known.

3. Experimental

A schematic of the experimental apparatus is shown in figure 2 and its calibration and performance are described in detail elsewhere [12]. The main features are as

follows: the sample is held in a thermostatically controlled temperature jacket ($\Delta T = \pm 0{\cdot}1°C$) and illuminated with light from a Coherent Innova 90 Ar^+ laser which is intensity modulated at 1 kHz. The laser filter removes stray plasma lines from the input beam. The illuminating and collection optics are $\times 50$ infinity-corrected microscope objectives. The resultant small spot size ($\approx 3\ \mu m$) allows for study on a micron scale and the large numerical aperture (0·6) ensures efficient collection of the incoherently scattered Raman shifted light. The notch filter removes the unshifted Rayleigh scattered light and the residue of the incident laser beam. The spectrometer is a Spex 1402 double monochromator incorporating a polarization scrambler. The lock-in amplifier (LIA) acts as an efficient noise rejection system and may be used to reject fluorescence [8, 20]. The VELA (Versatile Laboratory Instrument) digital memory device accumulates the data. This is driven by a BBC microcomputer, which also controls the application of the electric field to the sample. A time delay between consecutive AC electric field pulses was introduced to ensure that the alignment returned to its original planar state between pulses. The data acquisition system has a resolution of 100 μs per point.

The liquid crystals used in this study were the 4-*n*-alkyl-4′-cyanobiphenyl (*n*CB) homologues with $n = 5, 6, 7$ and 8 which all have nematic phases greater than 2°C wide. This ensured that post transitional phenomena in the nematic phase due to the isotropic phase would not dominate the results obtained. In the case of 8CB there is also an S_A phase at lower temperatures which allows pretransitional effects to be studied in the nematic phase as the S_A phase is approached. The materials were provided by BDH (now Merck UK) and used without further purification. Nematic to isotropic transition temperatures were determined to $\pm 0{\cdot}1°C$ using a microscope and hotstage.

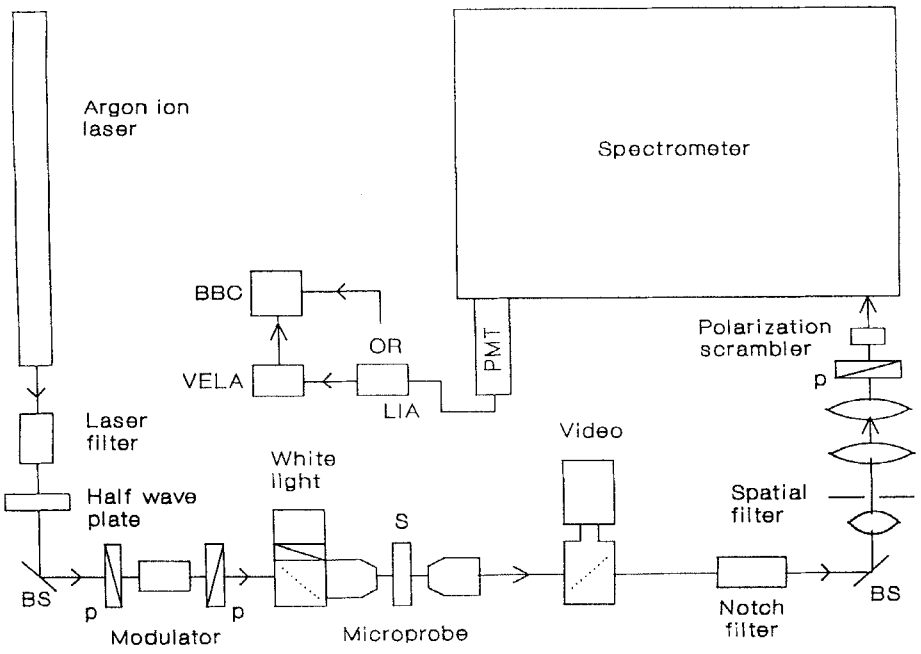

Figure 2. A schematic of the time resolved Raman microprobe apparatus. Symbols are BS, beam steerers; S, sample; p, polarizers.

The nematic materials were aligned in a planar texture using rubbed polyimide surfaces in cells whose sample thickness d was determined to an accuracy of $\pm 0{\cdot}1\ \mu m$ using interference techniques. The thickness was typically $14\ \mu m$. The cells included ITO electrodes so that electric fields could be applied across the sample in the direction of the incident laser beam, and in the quiescent state **n** was aligned parallel to the input laser light polarization direction.

The dominant bands relating to the rigid core section of the alkyl cyanobiphenyls [21] are due to the C≡N stretch (CN) centred at $2224\ cm^{-1}$, the C–C breathing of the aromatic rings (CC) at $1606\ cm^{-1}$, the C–C stretch of the biphenyl (CCB) at $1285\ cm^{-1}$ and the C–H in-plane deformation (CH) at $1185\ cm^{-1}$. The scattered Raman intensity, as a function of time for different applied field strengths, was accumulated for each of these bands at one reduced temperature for each homologue. One band, due to deformation of a specific bond, was then selected (see later) as a representative for a full temperature dependent study of k_{11} and η_{splay}. The alkyl chains (ALK) have their strongest band in the spectrum at $826\ cm^{-1}$. This was therefore used for a limited study of these parameters derived from the signal due to the alkyl chains. Following in outline the technique described previously [18] the recorded time dependent decrease of the Raman signal, in response to the applied field, was computer fitted to the analytical expression of equation (3) to determine S, the inverse response time. A typical response curve is given in figure 3. For a given voltage the constants A and B may be extracted from the data. Values of S and C are then suggested and an iterative computer fit carried out to maximize goodness of fit [12]. Curve fitting was deemed to be satisfactory when the consistency of S was within 0·1 per cent via the iterative process and 3 per cent for any two consecutive data fits. This goodness of fit can be clearly seen in the comparison between data and the curve fit to equation (3) in figure 3. Thus S (and A, B, and C) were determined for each applied voltage V. From linear plots of S versus V^2, η_{splay}, V_c and hence k_{11} were determined. In principle C could be used, in conjunction with $\psi_m^2(\infty)$ to determine ξ^2. However, the uncertainties in these numbers close to V_c preclude a sensible calculation of ξ being made. The values of $\Delta\varepsilon$ used in the calculations were those determined by Bradshaw and Raynes [11]. In order to ensure that the analytical expression was valid, i.e. in the limit of small deformations, the

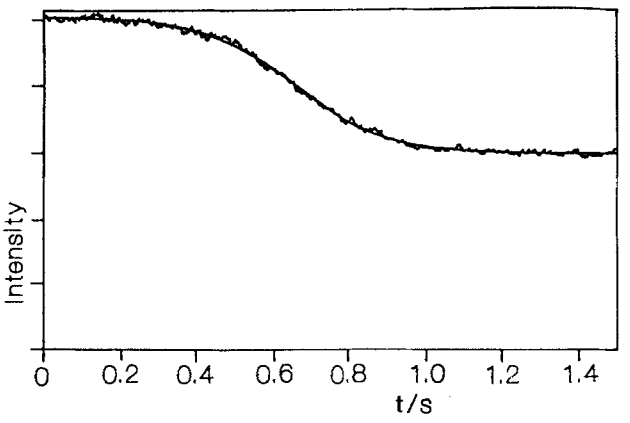

Figure 3. A typical transient Raman signal for 5CB at 24·6°C with an applied voltage (at $t=0$) of 1·1 V_{rms} and sine wave frequency of 1 kHz. The solid line is the fit of equation (3) to the experimental data.

applied voltages were always less than or equal to twice the critical voltage [22], in which case good fits to equations (3) and (4) were always obtained. Outside of this voltage range the data could not be fitted to these equations and this marks the upper limit of applicability of the theory. In earlier work [23] we showed that both the field-on and field-off response times could be determined. It was shown that the field-off response time was independent of V. In the present work we have concentrated on the field driven response times because this also enables V_c to be determined, at infinite response times, and hence k_{11} from the dependency of S on V_{rms}^2.

4. Results

4.1. *The core bands*

Following the experimental procedures which we have outlined the inverse response times, S, at a fixed temperature, were measured as a function of voltage, V_{rms}, for each of the core bands, (see figure 4). Each band, gives therefore, a separate probe of the voltage induced Fréedricksz transition. From figure 4 it is clear that, over the voltage range used, equation (4) fits the data well for each band. These data were then used to determine the apparent splay viscosities, critical voltages and splay elastic constants for the independent measurements on each of the core bands of 6, 7 and 8CB at the reduced temperatures indicated (see tables 1 (*a*)–(*c*)). Similar data for 5CB are presented elsewhere [12]. The estimated errors in η_{splay} are due in part to limitations in the fitting program which gives a maximum uncertainty of 3 per cent. The larger uncertainties in V_c (and therefore k_{11}) are due to the very small relative signal changes associated with the small deformation criterion, and hence difficulties in accumulating and extrapolating analysable data very close to V_c. The straight line dependencies were determined from the data using a least-squares fitting routine [12]. We did not force fit the data to the same V_c for the core bands. The small variation in V_c for each of the core bands which is reflected in the accuracy quoted in tables 1 and 2, illustrates the consistency of the measurements since we would expect the rigid core bands to give exactly the same V_c. Force fitting the data to the same or a mean V_c would induce an additional error of ~ 2 per cent in η_{splay}. Within the quoted errors, each independently

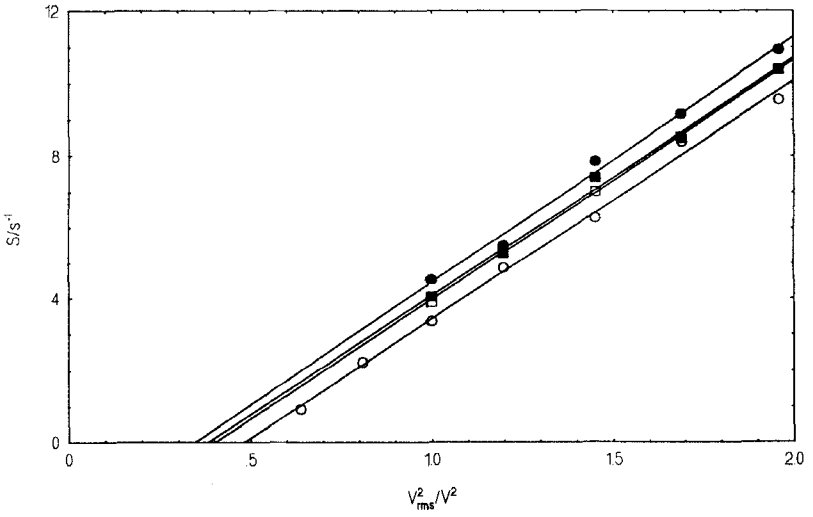

(*a*)

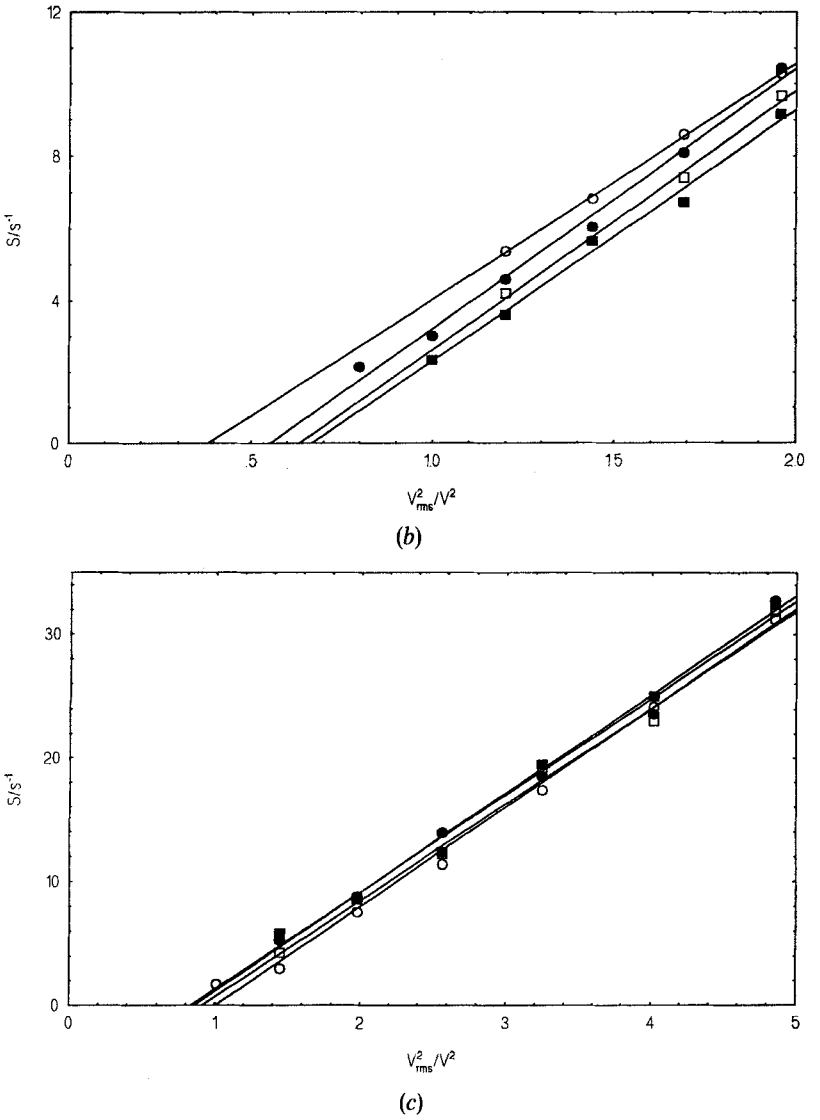

Figure 4. Inverse response time S versus applied rms voltage squared at shifted temperatures ($T_{NI} - T$) of 9·9°C, 13·4°C and 6·6°C, respectively, for each of the core bonds of the 6, 7 and 8CB homologues, (*a*) 6CB, (*b*) 7CB, (*c*) 8CB. ● CCB, ■, CH; □, C≡N; ○, C–C.

measured core band for each individual homologue shows good self-agreement and so we have also given the mean core values in these tables. Similar agreement was found for the core bands of 5CB [12]. Consequently following the agreement between core band signals it was appropriate to select a single band as representative of the core response to the applied electric field and use this to study the temperature dependence of the apparent viscosity coefficients and elastic constants in more detail. The C≡N stretch at 2224 cm^{-1} was chosen for further study. This is a bond, which incorporates the strong dipole moment whose interaction with **E** accounts for most of the torque when the field is first applied. It is reasonable to expect this bond to reorient at the same

rate as the director during the electric field induced Fréedericksz transition. This bond is also closely linked to the first phenyl ring and was the second most Raman active band of the four core bands. Thus it was suitably intense while showing results that represented the mean of the data for the core bands. The uncertainty in V_c is reflected in the errors quoted in k_{11}.

Table 1. Experimental data for the four independently measured core bands of the 6, 7 and 8CB homologues shifted temperatures ($T_{NI}-T$) of (*a*) 9·9°C, (*b*) 13·4°C and (c) 6·6°C, respectively. Core mean data represent average values characterizing the continuum properties.

Band	η_{splay}/cP	V_c/V	$k_{11}/10^{-12}$ N
CN	131±11	0·64±0·09	4·8±0·7
CC	134±12	0·69±0·06	4·9±0·4
CCB	133±12	0·62±0·14	3·8±0·9
CH	130±11	0·59±0·16	3·5±0·9
Core mean	132±11	0·63±0·11	4·0±0·7

(*a*) 6CB.

Band	η_{splay}/cP	V_c/V	$k_{11}/10^{-12}$ N
CN	121±11	0·81±0·08	6·6±0·7
CC	134±12	1·01±0·28	8·2±1·1
CCB	120±11	0·75±0·08	5·7±1·1
CH	125±11	0·82±0·11	6·8±0·9
Core mean	125±10	0·85±0·10	8·6±1·0

(*b*) 7CB.

Band	η_{splay}/cP	V_c/V	$k_{11}/10^{-12}$ N
CN	97±9	0·95±0·13	7·6±1·1
CC	94±8	1·00±0·12	8·3±1·0
CCB	97±9	0·90±0·15	6·8±1·2
CH	95±8	0·92±0·13	7·1±1·0
Core mean	96±8	0·94±0·13	7·9±1·0

(*c*) 8CB.

Table 2. V_c data for the C≡N band of the cyanobiphenyl homologues.

6CB		7CB		8CB	
$(T_{NI}-T)$/°C	V_c/V	$(T_{NI}-T)$/°C	V_c/V	$(T_{NI}-T)$/°C	V_c/V
9·8	0·64±0·13	13·4	0·81±0·10	6·6	0·95±0·16
7·9	0·70±0·12	11·4	0·84±0·12	5·6	0·89±0·14
5·8	0·67±0·10	9·1	0·87±0·16	4·6	0·83±0·17
3·7	0·65±0·14	7·4	0·81±0·15	3·5	0·88±0·13
1·7	0·69±0·09	5·4	0·75±0·17	2·5	0·81±0·12

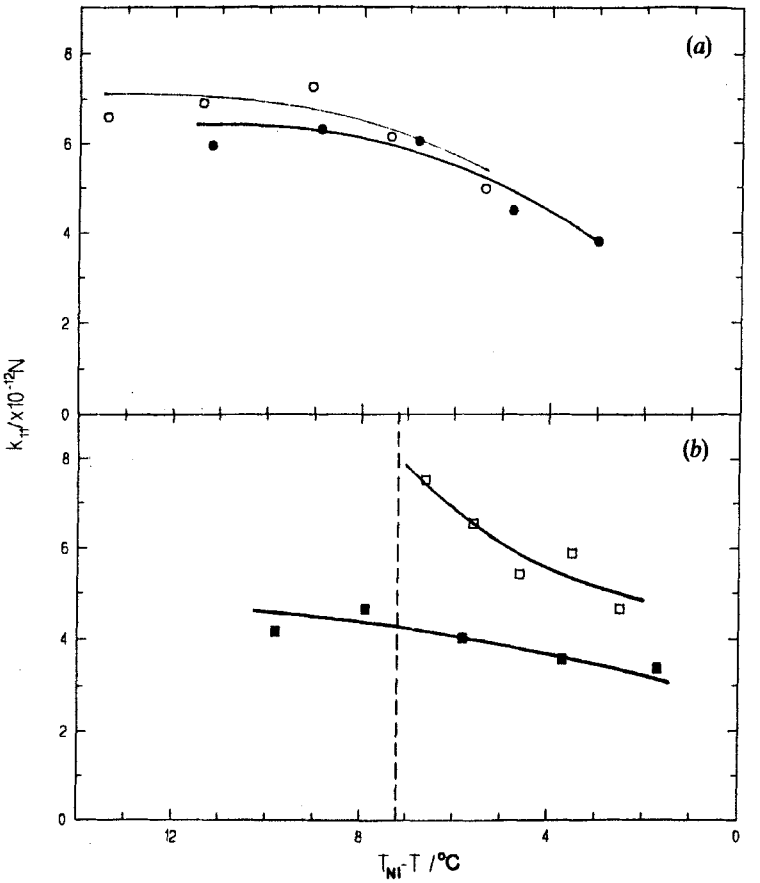

Figure 5. The variation of k_{11} as a function of shifted temperature for (*a*) 5CB (●) and 7CB (○), (*b*) 6CB (■) and 8CB (□) as determined using the Raman microprobe. The dashed line shows T_{S_AN} for 8CB.

4.2. *The cyano stretch*

Figure 5 shows the variation in k_{11} with temperature for the semi-rigid core, or C≡N stretch, of the homologues. Similarly determined and previously unpublished elastic constant data for 5CB are included here. Before considering the data further it is useful to note that the results agree well with those recorded by dynamic light scattering [9] and electric and magnetic Fréedericksz transition techniques [11]. The present data, derived from the C≡N bond motion, for 5, 6 and 7CB agree on average to within 10 per cent and for 8CB to within 2 per cent of the reported values in [9] and [11]. The V_c data from which the values of k_{11} are determined are listed for comparison in table 2. The present data show the expected decrease in the elastic constant as the nematic to isotropic transition is approached. On the other hand as the temperature decreases the elastic constants for 5, 6 and 7CB tend to increase slowly to a plateau whilst those for 8CB appear to increase more strongly near the N–S_A phase transition. The results for the odd members (5 and 7) are very similar whilst those for the even members (6 and 8) underline the differences recorded when there is a low-lying smectic phase [24]. These results, which agree with previous data, illustrate the usefulness and sensitivity of the present technique.

The twist, γ_1, and splay, η_{splay}, viscosities of a liquid crystal are linked through

$$\eta_{splay} = \gamma_1 - (\alpha_3^2/\eta_b),$$

where α_3 is a Leslie coefficient and η_b is a Miesowicz viscosity. For nematic materials it has been shown experimentally that $\eta_{splay} = \gamma_1$ provided that pretransitional effects are not present [9, 24]. Thus the results for η_{splay} and γ_1 are equivalent for 5, 6 and 7CB. In the case of 8CB, η_{splay} and γ_1 show a divergence as the S_A phase is approached on decreasing the temperature. Since twist fluctuations are forbidden in the S_A phase γ_1 diverges strongly. On the other hand η_{splay} is finite in the S_A phase. Thus the (α_3^2/η_b) term becomes measurable at the N to S_A phase transition since η_{splay} diverges less rapidly than γ_1 [9, 24]. Figure 6 (*a*) shows the variation of the splay viscosity with temperature determined for the C≡N stretch from the S versus V^2 data (see figure 4). In the light scattering study [9, 24] a comparison was carried out between the different measuring techniques used for the determination of the viscosity coefficients. Generally, reasonable agreement, with 7 per cent, was found between the light scattering data and those determined by Zvetkow rotating field techniques [10, 25]. Comparative data from [9], are presented in figure 6 (*b*). In comparison, the data for 6 and 8CB are, on average, within 4 per cent and 2 per cent, respectively, of the light scattering data, whilst those of 5 and 7CB are some 20 per cent higher. It is difficult to explain these differences,

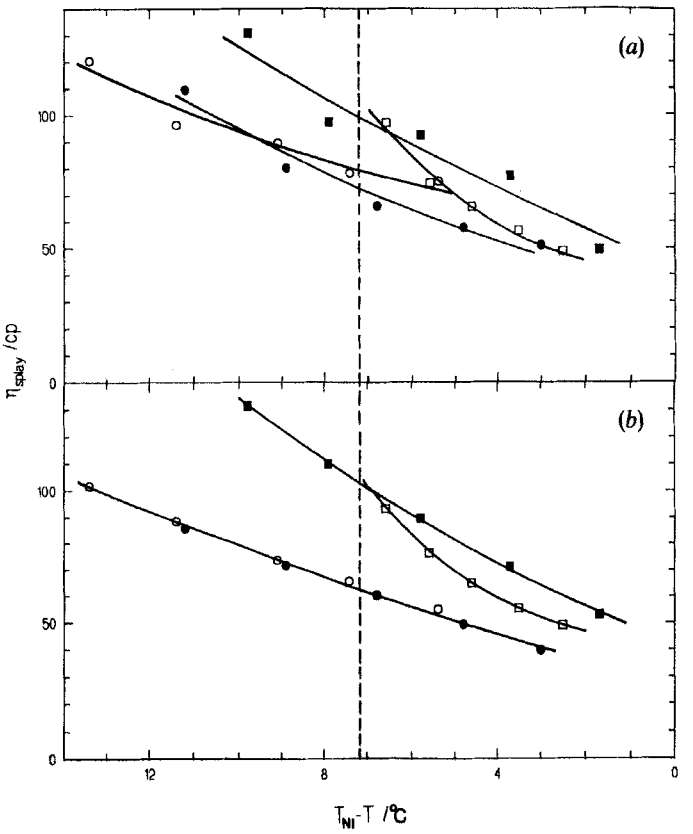

Figure 6. The variation of η_{splay} as a function of shifted temperature for 5–8CB determined by (*a*) the Raman microprobe and (*b*) electric field light scattering [9]. The dashed line shows T_{S_AN} for 8CB. ■, 6CB; ○, 7CB; □, 8CB; ●, 5CB.

however, it is interesting to note the consistent behaviour of the even and odd members of the series. This may point to a molecular origin for the differences between the light scattering and Raman results. The former probes the overall average polarizability of the whole molecule whilst the latter probes the change in polarizability associated only with the C≡N stretch. All data are calculated in the limit of small deformations. A comparison of both data sets (see figures 6 (*a*) and (*b*) shows that, (i) the even members have a consistently higher splay viscosity than the odd members, (ii) the shapes of the viscosity curves are similar, implying the same type of Arrhenius behaviour, (iii) the activation energies of the even members are higher than those of the odd members, and (iv) in the case of 8CB, with the low-lying S_A phase, the splay viscosity diverges as the transition is approached. Thus the time resolved Raman microprobe technique demonstrates the same data trends as the more conventional measuring techniques independent of the homologue under study.

4.3. *The alkyl chain bands*

The strongest chain band is nearly two orders of magnitude less intense than the most intense of the core bands and lies close to a ring breathing vibration. Accumulation of data from this band was therefore difficult and extremely slow. However, a preliminary study was carried out for each homologue at the same shifted temperature ($T_{NI} - T = 3°C$) and data for apparent values of η_{splay} and k_{11} extracted using the same method as for the C≡N stretch, i.e. from the dependence of S on V^2 (see figure 7). From the slope of this graph it is clear that, in the limit of small deformations, the alkyl chain has a much faster response time than the rigid core. The threshold voltage is, however, lower for the rigid core and these data combined suggest complex initial deformation and dynamics are involved in the initial reorientation mechanisms of nematic liquid crystals when subject to a Fréedericksz transition. We have recorded similar data for the other homologues, 6, 7 and 8CB. A comparison of the alkyl chain

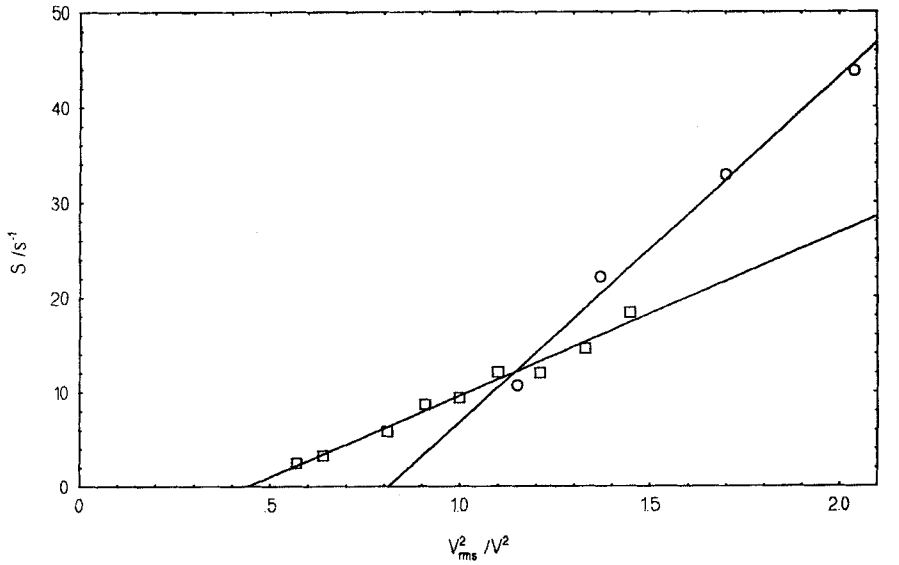

Figure 7. Inverse response times versus applied rms voltage squared at a shifted temperature of 3°C for the rigid C≡N stretch band (□) and the alkyl chain bands (○).

Table 3. Apparent viscosity coefficient and elastic constant data for the alkyl chains of the four homologues at a shifted temperature of 3°C.

*n*CB	η_{splay}(ALK)/cP	η_{splay}(CN)/cP	K_{11}(ALK)/10^{-12} N	K_{11}(CN)/10^{-12} N
5	24±3	53±5	7·6±1·2	4·1±0·6
6	39±2	61±6	6·3±3·8	3·4±0·5
7	26±5	69±6	4·4±2·4	4·3±0·7
8	21±2	50±5	5·3±1·5	3·3±0·5

and C≡N data is given in table 3. From this table it can be seen that the apparent η_{splay} determined from the signal associated with the flexible alkyl chains is, on average, consistently a factor of two times smaller than that associated with the C≡N bond for all four homologues. This is well outside of any experimental error. The elastic constants on the other hand appear to be high for the alkyl chain derived signal. Without a detailed temperature dependent study it is difficult to analyse the data further. It is clear that the Raman technique, which is inherently site selective, gives rise to different constants determined from signals associated with rigid (core) and flexible (alkyl chain) molecular components for small field induced deformations.

5. Conclusions

In the present work a low noise, time resolved Raman microprobe has been used to study the Fréedericksz transition for members of a homologous series of nematic compounds aligned initially with a planar surface texture. The microprobe apparatus records the Raman signal associated with a specific bond or deformation within the molecule. It is intrinsically site selective and gives rise to a spectral line associated with a particular part of the molecule, i.e. the semi-rigid core –C≡N (see [12 (a), p. 150)] stretch, C–C breathing mode, etc., or the flexible alkyl chain. The change in intensity of a specific spectral line has then been studied, as a function of time, in response to an applied external field. For all four nematogenic alkylcyanobiphenyl homologues we have observed a remarkedly consistent response for Raman active sites associated with the semi-rigid molecular core for each homologue. From the response times, in the limit of small deformation, and from the threshold voltages we have determined values for the effective splay elastic constants and viscosity coefficients. These data are self-consistent and slightly higher than those recorded using currently accepted techniques based on rigid rod polarizability ellipsoid models (i.e. optical or dielectric methods). The core data show distinct odd–even effects and classical temperature dependencies. In the case of 4-*n*-octyl-4′-cyanobiphenyl the viscosity data shows distinct pretransitional behaviour as the lower lying smectic A phase is approached. Similarly the elastic constant data demonstrate a more marked temperature dependence than 4-*n*-hexyl-4′-cyanobiphenyl which does not have an S_A to N phase transition. Thus, it is clear that the Raman microprobe technique can be used reliably to study the properties and behaviour of nematic liquid crystals at least with signals derived from the semi-rigid core. In the case of the alkyl chain signals the results show significant trends and features. The response times, in the limit of small deformations, are consistently faster, by a factor of two, with respect to those associated with the semi-rigid core signals. Following the Pieranski analysis this implies a lower apparent viscosity and, from the threshold voltages, different apparent elastic constants for the alkyl chains and the rigid aromatic core. Since the detection and treatment of data are the same irrespective of the frequency of the recorded spectral line, the difference in response times, must be real.

Also the data are consistent for all four homologues. Thus we are forced to conclude that signals associated with rigid and flexible molecular sites which probe different director averages give rise to different dynamic and static information. It is interesting to note that the semi-rigid core and flexible alkyl chain data lead to higher and lower values, respectively, of the apparent viscosity coefficients with respect to those recorded by classical methods, that treat the molecule as a rigid sub-unit and assume a mean field. We are left with the inescapable conclusion that, in the limit of small deformations, it is possible to record, using the time resolved Raman microprobe, on a macroscopic scale, the effects of molecular flexibility in response to an applied external field. This suggests the need for new theories based on flexible rather than rigid rod models to explain dynamics of nematogenic systems.

Finally, it is worth stressing the advantages of the Raman microprobe technique. It is chemically site selective and time resolved (down to 100 μs). It uses micron sized sample volumes as well as low laser powers, and has spatial resolution on the micron length scale. Utilization of the phase sensitive detection method and notch filter system allow virtually pure Raman spectra to be obtained. The present microprobe was a relatively expensive spectrometer system and so the method might have less appeal at first sight than more conventional macroscopic techniques. These will not, however, have the inherent bond selectivity of the Raman technique. Further we are currently developing a new low cost multilayer dielectric filter spectroscopic system [26] that will enhance the sensitivity and precision whilst incorporating all the above advantages. This will allow us to measure dynamic phenomena with much greater accuracy for the rigid and flexible bands close to V_c and thereby gain a better understanding of the dynamics of nematic liquid crystals.

We thank the S.E.R.C. for the award of a studentship (K.M.B.) and Research Grant (GR/B/88174) (H.J.C.). We also thank the late Dr Ben Sturgeon for support through the provision of samples and enthusiastic interest in the work.

References

[1] LEWIS, A. L., SPOOHOWER, J., BOGOMOLNI, R. A., LOZIER, R. H., and TOCHENQUIS, W., 1979, *Proc. natn. Acad. Sci., U.S.A.*, **71**, 4462.
[2] CHANG, R. K., 1983, *J. Phys., Paris*, **44**, 283.
[3] GRUNEISEN, M. T., MACDONALD, K. R., and BOYD, R. W., 1988, *J. opt. Soc. Am.* B, **5**, 123.
[4] KUROSAWA, K., SASAKI, W., FUJIWARE, E., and KATO, Y., 1988, *I.E.E.E. Jl quant. Electron.*, **24**, 1908.
[5] GERRARD, D. L., and BOWLEY, H. J., 1986, *Poly. Commun.*, **27**, 43.
[6] ROSASCO, G. J., ROEDDER, E., and SIMMONS, J. H., 1975, *Science, N. Y.*, **190**, 557.
[7] ROSASCO, G. J., and ETZ, E., 1975, *Appl. Spectrosc.*, **29**, 396.
[8] COLES, H. J., 1986, *Phys. Bull.*, January, p. 10.
[9] COLES, H. J., and SEFTON, M. S., 1985, *Molec. Crystal liq. Crystals Lett.*, **1**, 151, 1985, *Ibid.*, **1**, 159; 1986, *Ibid.*, **3**, 63; *Liq. Crystals* (in the press).
[10] SIEDLER, L. T. S., HYDE, A. J., PETHRICK, R. A., and LESLIE, F. M., 1983, *Molec. Crystal liq. Crystals*, **90**, 225.
[11] BRADSHAW, M. J., RAYNES, E. P., BUNNING, J. D., and FABER, T. E., 1985, *J. Phys., Paris*, **46**, 1513.
[12] (a) BOOTH, K. M., 1988, Ph.D. Thesis, University of Manchester. (b) BOOTH, K. M., NASH, J., and COLES, H. J., 1992, *Meas. Sci. Tech.*, **3**, 843.
[13] JEN, S., CLARK, N. A., PERSHAN, P. S., and PRIESTLY, E. B., 1973, *Phys. Rev. Lett.*, **31**, 1552; 1977, *J. chem. Phys.*, **66**, 4635.
[14] MIYANO, K., 1977, *Phys. Lett.* A, **63**, 37; *J. chem. Phys.*, **69**, 4807.
[15] HEGER, J. P., 1975, *J. Phys. Lett., Paris*, **36**, L-209.
[16] SEELIGER, R., HASPEKLO, H., and NOACK, F., 1983, *Molec. Phys.*, **49**, 1039.

[17] DALMOLEN, L. G. P., PICKEN, S. J., DE JONG, A. F., and DE JEU, W. H., 1985, *J. Phys., Paris*, 1443.
[18] PIERANSKI, P., BROCHARD, F., and GUYON, E. J., 1973, *J. Phys., Paris*, **34**, 35.
[19] LONG, D. A., 1977, *Raman Spectroscopy* (McGraw-Hill).
[20] DEMAS, J. N., and KELLAR, P. A., 1985, *Analyt. Chem.*, **57**, 545.
[21] GRAY, G. W., and MOSLEY, A., 1976, *Molec. Crystals liq. Crystals*, **35**, 71.
[22] WELFORD, K. R., and SAMBLES, J. R., 1987, *Molec. Crystals liq. Crystals*, **147**, 25.
[23] COLES, H. J., and TIPPING, J., 1985, *Nature*, **316**, 136; 1985, *Molec. Crystals liq. Crystals*, **2**, 23.
[24] COLES, H. J., and SEFTON, M. S., 1987, *Molec. Crystals liq. Crystals*, **4**, 123.
[25] BOCK, F.-J., KNEPPE, H., and SCHNEIDER, F., 1986, *Liq. Crystals*, **1**, 239.
[26] BATCHELDER, D. N., CHENG, C., and PITT, G. D., 1991, *Adv. Mater.*, **3**, 566.